MASS TRANSFER MECHANISM OF DEIONIZATION BY MIXED BED

TAKESHI KATAOKA, AKINORI MUTO AND
TADAAKI NISHIKI

Department of Chemical Engineering, College of Engineering,
University of Osaka prefecture, Sakai, 593

For deionization by a mixed bed, a mass transfer model is presented on the basis of both cation and anion exchange reactions and neutralization reaction. Cation and anion exchange characteristics and mixed fraction of the two resins are considered in the model.

Theoretical ionic breakthrough curves of the model equations were obtained by using a finite difference numerical method. Effects of salt, concentration, flow rate of feed solution, bed height and mixed fraction of both resins on the breakthrough curves were examined theoretically and experimentally. The calculated breakthrough curves agreed with experimental data under various conditions. This result suggests that the proposed model can be applied to the deionization process in a mixed bed. The relation between the diffusion resistances of transfer ions and the operational conditions was also studied using a numerical simulation.

Introduction

Mixed bed operation is very effective for deinoization of water. This operation has been practically used as one of the important processes to produce ultra pure water. The deionization process using a mixed bed has been examined on the basis of experimental results[1, 12]. It is nesessory to elucidate details of the deionization mechanism in order to satisfy requirements for both high quality and quantity of ultra pure water. Recently, Haub and Foutch[2] presented a mass transfer model in a mixed bed on the basis of elemental reactions. Their theoretical expressions were derived with respect to the removal of NaCl under liquid phase diffusion controlling. In practice, their model may only be applicable to limited conditions.
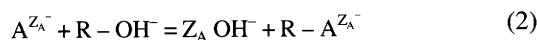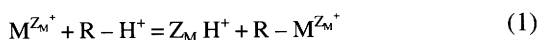
A more practical model which contained ionic valence, diffusion resistances in both liquid and resin phases and mixed volume ratio of the two resins was presented[5]. The stirred tank experimental data showed that this mass transfer model could express the deionization process.

In our present study, this mass transfer model is applied to mixed bed operation. The separation mechanism in a mixed bed is discussed on basis of theoretical and experimental results.
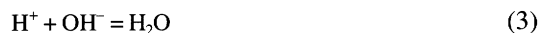
1. Theory

1.1 Basic expressions

Removal of salt using a mixed bed which consists of $M^{Z_M^+}$ and $A^{Z_A^-}$, proceeds via the following two ion exchange and neutralization reactions.

$$M^{Z_M^+} + R - H^+ = Z_M H^+ + R - M^{Z_M^+} \tag{1}$$

$$A^{Z_A^-} + R - OH^- = Z_A OH^- + R - A^{Z_A^-} \tag{2}$$

$$H^+ + OH^- = H_2O \tag{3}$$

Mass transfer of ions in the mixed bed on the basis of Eqs. (1) - (3) is described below.

Mass balance equations for differential heights of the mixed bed for each ion, $M^{Z_M^+}$ and $A^{Z_A^-}$, are shown by Eqs. (4) and (5), respectively, neglecting dispersion along the column axis.

$$\frac{U_f}{\varepsilon}\left(\frac{\partial x_M}{\partial z}\right) + \left(\frac{\partial x_M}{\partial t}\right) + \left(\frac{1-\varepsilon}{\varepsilon}\right)m_H\left(\frac{Q_H}{C_{M,f}}\right)\left(\frac{\partial \bar{y}_M}{\partial t}\right) = 0 \tag{4}$$

$$\frac{U_f}{\varepsilon}\left(\frac{\partial x_A}{\partial z}\right) + \left(\frac{\partial x_A}{\partial t}\right) + \left(\frac{1-\varepsilon}{\varepsilon}\right)(1-m_H)\left(\frac{Q_{OH}}{C_{A,f}}\right)\left(\frac{\partial \bar{y}_A}{\partial t}\right) = 0 \tag{5}$$

where U_f and ε denote the flow rate of a solution and the porosity of the mixed bed, respectively. Q is the ion exchange capacity of the resin and C_f is the concentration of feed solution. m_H indicates the volume fraction of H-type resin in the mixed resins.

The mass transfer equations for ions were derived by applying Nernst-Planck's equation to diffusion processes in both liquid and resin phases.

The details of the equations are described in a previous paper[5].

The values of liquid phase mass transfer coefficients of an ion in a bed are evaluated by the correlation on basis of the hydroraulic radius model[6, 7] (Eqs. (6) and (7)).

$$j_L' = \left(\frac{1-\varepsilon}{\varepsilon}\right)^{1/3}\left(\frac{K_L^0 Sc^{2/3}}{U_f/\varepsilon}\right) = 1.85\,Re'^{-2/3} \tag{6}$$

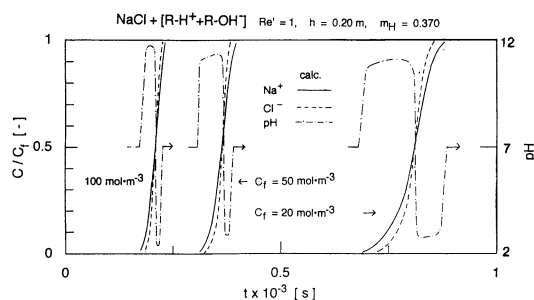$$\frac{k_L}{k_L^0} = \left(\frac{D_e}{D}\right)^{2/3} \tag{7}$$

NaCl + [R-H⁺+R-OH⁻]   Re' = 1,   h = 0.20 m, m_H = 0.370

Fig. 1 Simulated breakthrough curves for Na⁺ and Cl⁻, and pH of effluent

where

$$\mathrm{Re'} = \frac{d_p\, U_f\, \rho}{(1-\varepsilon)\eta} \tag{8}$$

$$\mathrm{Sc} = \frac{\eta}{\rho D} \tag{9}$$

The meanings of these symbols in the above equations are shown in the nomenclature section.

We calculated the ionic breakthrough curves by the finite difference method. The Cranck - Nicolson method was applied to the resin phase diffusion process. The explicit differencial method was applied to the liquid phase one and the mass balance equations. The calculations were made under the condition that each ion's fluxes in both liquid and resin phases were kept equal at the liquid - resin interface. The flux of the ions in the liquid phase was obtained depending on the pH value of the liquid bulk phase. (Refer to Eqs. (22) and (23) in the previous paper[5].)

The following initial and boundary conditions are used in the calculation.

initial conditions $(t = 0)$;

$$q_M = q_A = 0 \; (0 < z < h) \tag{10}$$

$$C_M = C_A = 0 \; (0 < z < h) \tag{11}$$

boundary conditions;
column inlet $(z = 0)$

$$C_M = C_{M,f} \tag{12}$$

$$C_A = C_{A,f} \tag{13}$$

1.2 Simulation results

Typical simulated breakthrough curves of Na⁺ and Cl⁻ from the mixed bed are shown in **Fig. 1** under a feed concentration of $C_f = 100 - 20$ mol·m⁻³. The pH value of the effluent is also shown in the same figure. The values listed in the previous paper[5] and the measured values of the ion exchange capacities[4] were used in the simulation.

Both resins were mixed at equal normality, that is, $Q_H \nu_H / Q_{OH} \nu_{OH} = 1.0$, $m_H = 0.370$.

From the calculated results, Na⁺ is found to break through earlier than Cl⁻ in all feed solutions. This suggests that the anion exchange rate is faster than the cation exchange rate. Effluent becomes alkaline from the break-
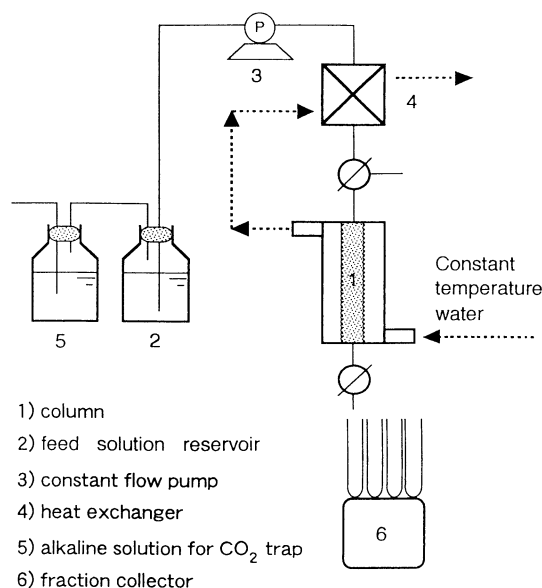

1) column
2) feed solution reservoir
3) constant flow pump
4) heat exchanger
5) alkaline solution for CO_2 trap
6) fraction collector

Fig. 2 Experimental apparatus

through point. After that, the concentrations of both ions in the effluent increase gradually. On the way, the concentration of Cl⁻ becomes larger than that of Na⁺. The effluent turns from alkaline to acidic. The pH fluctuation of the effluent becomes greater with increased concentration of feed solution.

2. Experimental

The two resins used were DIAION SK1B and SA10A manufactured by Mitsubishi chemical Corp. The resins, which were sieved before the experiment, were conveted into H-type and OH-types, respectively, using usual conditioning methods. Apparatus for a column experiment is shown in **Fig. 2**. Both weighed resins were fully mixed and packed into the column (internal diameter 0.01 m) with a constant temperature water jacket. A feed solution was prepared by using extra pure reagents and degassed pure water. The feed solution was stocked in a plastic reservoir (2) into which gas washer with an alkaline solution for the absorption of CO_2 in the atmosphere was installed. The solution was fed into the column at constant flow rate. The effluent was collected by a fraction collector. The breakthrough curves were measured by concentration analysis of each ion in the effluent. All column experiments were carried out at 298 K. The concentration of cation was determined by emission- or plasma- spectrophotometory. The Cl⁻ concentration was measured by silver titration or ion chromatography method.

3. Results and Discussion

3.1 Breakthrough curves of ions and pH value of effluent

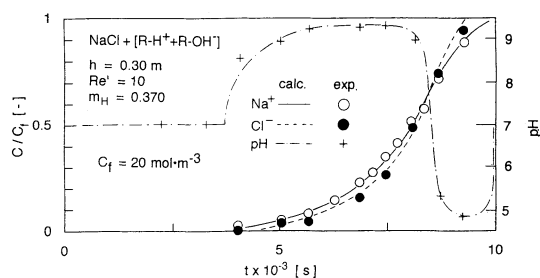Both calculated and experimental breakthrough curves of Na⁺ and Cl⁻ are shown in **Fig. 3**, when NaCl solu-

Fig. 3 Comparison of calculated lines and experimental data for NaCl + [R-H$^+$ + R-OH$^-$]
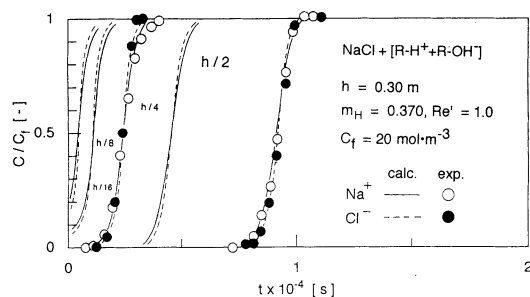

Fig. 4 Effect of bed height on breakthrough curves for NaCl

tion with a concentration of 20 mol·m^{-3} is fed into the mixed bed. These calculated curves were obtained by considering both liquid and resin diffusion resistances.

The theoretical lines of both breakthrough curves and pH value of the effluent shown in the figure agreed with the measured values. Thus, it is suggested that the presented mass transfer mechanism can express the breakthrough curves of each ion from the mixed bed.

3.2 Effect of bed height on breakthrough curves

The breakthrough curves of both Na$^+$ and Cl$^-$ under various bed heights are shown in **Fig. 4**. These curves were calculated by considering both liquid and resin diffusion resistances.

The calculated curves for Na$^+$ and Cl$^-$ respectively show a constant pattern near a column inlet. According to the calculation, both moving velocities of the concentration waves of Na$^+$ and Cl$^-$ become constant at $z = 5.85 \times 10^{-2}$ m under this operating condition. Because deionization by the mixed resin shows very "favorable" equilibria as a rectangular isotherm does[4], the concentration waves easily reach the constant pattern.

3.3 Effects of concentration and flow rate of the feed solution on the breakthrough curve

Figure 5 shows the breakthrough curves of Na$^+$ and Cl$^-$ from 0.30 m height of the mixed bed when $C_f = 20$ and 2.5 mol·m^{-3} and Re' = 10 and 1, respectively. Agreement between the experimental and calculated results support the assumption that the mass transfer model can be applied to various operating conditions. Theoretical breakthrough curves show a constant pattern in the same as Fig. 4, though we omitted to show it the figure.
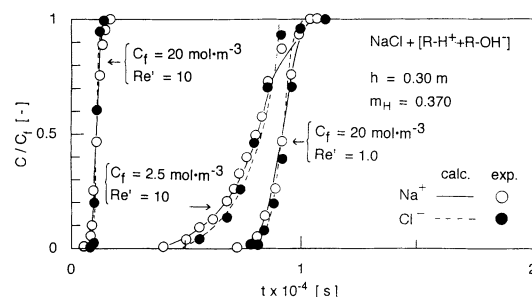

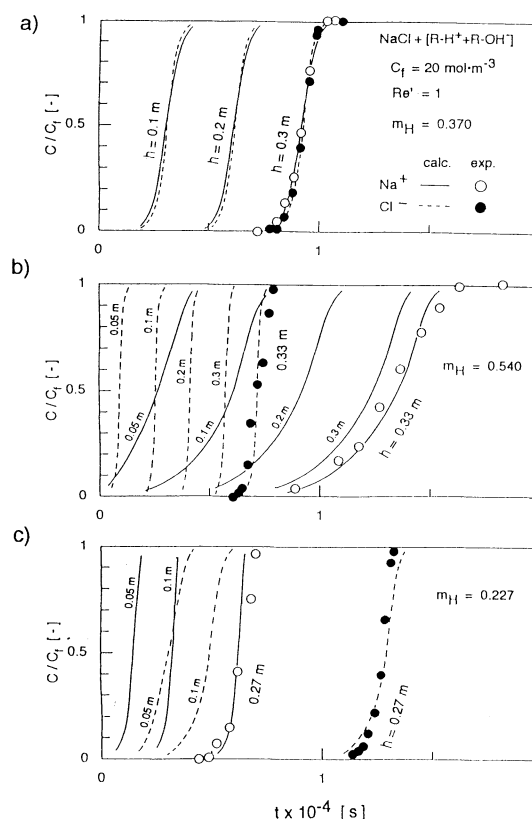**Fig. 5** Effect of concentration and flow rate of NaCl feed solution on breakthrough curves

Fig. 6 Effect of mixed ratio m_H on breakthrough curves of NaCl. a) $m_H = 0.370$, b) $m_H = 0.540$, c) $m_H = 0.227$

3.4 Effect of mixed volume fraction, m_H, on the breakthrough curves

Breakthrough curves under various values of m_H were measured with the total amount of ion exchange capability ($Q_H v_H + Q_{OH} v_{OH}$) kept constant. In three cases, namely, a) mixing both resins at equal normality ($Q_H v_H / Q_{OH} v_{OH} = 1.0$, $m_H = 0.370$), b) mixing more H-type resin and less OH-type resin ($Q_H v_H / Q_{OH} v_{OH} = 2.0$, $m_H = 0.540$), and C) mixing more OH-type resin and less H-type resin($Q_H v_H / Q_{OH} v_{OH} = 0.50$, $m_H = 0.227$), both calculated and experimental curves are shown in **Fig. 6**. In all cases, the calculated breakthrough curves of both Na$^+$ and Cl$^-$ establish a constant pattern regardless of the value of m_H. The measured breakthrough curves conformed to the
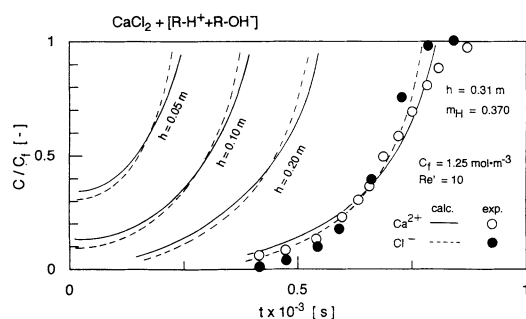
Fig. 7 Breakthrough curves for $CaCl_2$ + [R-H$^+$ + R-OH$^-$]

Fig. 8 Comparison of breakthrough curves of Na$^+$ and Cl$^-$ under liquid phase diffusion controlling with ones for considering both phase diffusion resistances

theoretical ones. The present model is applicable when both resins are mixed at non-equal normality.

3.5 Deionization of a multivalent ion by the mixed bed

The present model was also applied to deionization of a multivalent ion by mixed bed operation. The breakthrough curves of Ca^{2+} and Cl$^-$ are shown in **Fig. 7**. The theoretical lines for both ions agreed well with experimental data.

3.6 Relation between operational conditions and diffusion resistance

It is important to elucidate the relation between the operating conditions and diffusion resistance of ions in the mixed bed.

In NaCl + [R-H + R-OH] sytem, the typical breakthrough curves for C_f = 20 and 2.5 mol·m^{-3} under both liquid phase diffusion controlling and existence of both diffusion resistances are compared in **Fig. 8**. In the figure, σ is the ratio of liquid phase diffusion rate and resin phase one. The value of $\sigma_{H, M}$ is evaluated by

$$\sigma_{H, M} = \frac{\left(\dfrac{6k'_{L, H, M}}{d_p}\right) C_{f, M}}{\left(\dfrac{60 \, \overline{D}'_{H, M}}{d_p^2}\right) Q_H} \tag{14}$$

where $k'_{L, H, M}$ means liquid phase mass transfer coefficient on the basis of effective diffusivity initial state of cation exchange[8]. $\overline{D}'_{H, M}$ the value of the mutual resin phase diffusivities, is evaluated using resin phase self-diffusivities[9, 11]. The values of $\sigma_{OH, Cl}$ for anion exchange is also obtained in the same way.

From these calculated results, the mass transfer of ions in the mixed bed was found to be under liquid phase diffusion controlling when the value of σ is less than near 0.1.

Conclusion

The mass transfer model on the basis of both cation and anion exchanges and neutralization reaction was applied to a mixed bed. Effects of bed height, concentration of ions in feed solution, flow rate, the mixed volume ratio of the two resins and ionic valence on the breakthrough curves were examined. Good agreement between
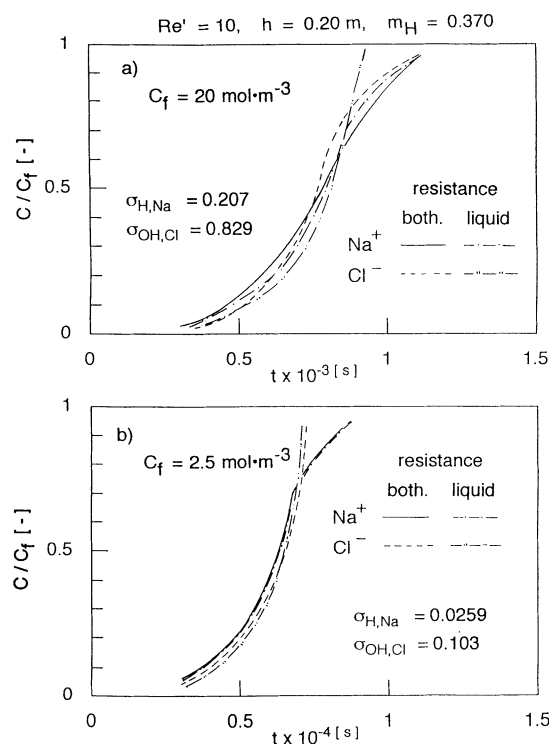
calculated and experimental results suggests that the model can be applied to mass transfer processes in a mixed bed. The parameter, σ, defined by Eq. (14) for diffusion resistances in both resin and liquid phases, was introduced. The calculation results showed that the deionization made progress under liquid phase controlling when $\sigma < 0.1$.

Nomenclature

C	=	concentration of ion in liquid phase	[mol·m^{-3}]
D	=	self - diffusivity	[m^2·s^{-1}]
D_e	=	effective diffusivity	[m^2·s^{-1}]
d_p	=	diameter of an ion exchange resin	[m]
h	=	bed height	[m]
j_L	=	j factor	[-]
K	=	ion exchange equilibrium constant	
k_L	=	liquid phase mass transfer coefficient with electric field	[m·s^{-1}]
k_L^o	=	liquid phase mass transfer coefficient without electric field	[m·s^{-1}]
k_L'	=	liquid phase mass transfer coefficient on the basis of effective diffusivity initial state of ion exchange	[m·s^{-1}]
m_H	=	mixed volume ratio (= v_H / (v_H + v_{OH}))	[-]
Q	=	ion exchange capacity	[mol·m^{-3}]
q	=	concentration of ion in resin phase	[mol·m^{-3}]
$\bar{q}$	=	average concentration of ion in resin phase	[mol·m^{-3}]
Re'	=	modified Reynols number	[-]
v_H	=	volume of a H-type resin in a mixed bed	[m^3]
v_{OH}	=	volume of a OH-type resin in a mixed bed	[m^3]
Sc	=	Schmidt number	[-]
t	=	time	[s]
U_f	=	superficial velocity	[m·s^{-1}]
x	=	C / C_f	[-]
y	=	q / Q	[-]
Z	=	ionic valence	[-]

z	=	distance of a column inlet	[-]
α	=	D_H / D_M	[-]
β	=	D_{OH} / D_M	[-]
ε	=	void fraction of a bed	[-]
η	=	kinematic viscosity	$[m^2 \cdot s^{-1}]$
ρ	=	density of fluid phase	$[kg \cdot m^{-3}]$
$\sigma_{H,M}$	=	parameter defined by Eq. (14)	[-]

\<subscript\>

A	=	anion to be removed
b	=	liquid bulk phase
f	=	feed solution
H	=	H^+
M	=	cation to be removed
OH	=	OH^-
R	=	reaction plane

\<superscript\>

-	=	resin phase
~	=	resin-liquid interface

Literature Cited

1) Frisch N. W. and R. Kunin: *AIChE J.*, **6**, 640-647(1960)
2) Haub C. E. and G. C. Foutch: *Ind. Eng. Chem. Res.*, **25**, 373-381 (1986)
3) Helfferich F. and M. S. plesset: *J. Chem. Phys.*, **28**, 418-424(1958)
4) Kataoka T., A. Muto and T. Nishiki: *J. Chem. Eng. Japan*, **26**, 644-648 (1993)
5) Kataoka T., A. Muto and T. Nishiki: *J. Chem. Eng. Japan* **27**, 375-381 (1994)
6) Kataoka T., H. Yoshida and K. Ueyama: *J. Chem. Eng. Japan*, **5**, 132-136 (1972)
7) Kataoka T., H. Yoshida and T. Yamada: *J. Chem. Eng. Japan*, **6**, 172-177 (1973)
8) Kataoka T. and H. Yoshida: *J. Chem. Eng. Japan*, **9**, 383-387 (197
9) Kataoka T., H. Yoshida and Y. Ozasa: *J. Chem. Eng. Japan*, **10**, 385-390 (1977)
10) Kataoka T. and K. Ueyama: *J. Chem. Eng. Japan*, **1**, 38-42 (1968)
11) Rao M. G. and M. M. David: *AIChE J.*, **10**, 213-219 (1964)
12) Reents A. C. and F. H. Kahler: *Ind. Eng. Chem., Fundam.*, **43**, 730-734 (1951)